Accepted Manuscript

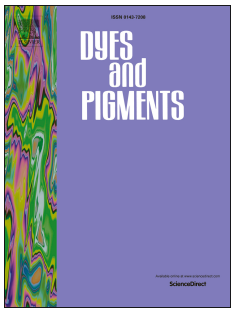

Heavy-atom-free charge transfer photosensitizers: Tuning the efficiency of BODIPY in singlet oxygen generation via intramolecular electron donor-acceptor interaction

Wenbin Hu, Yanhe Lin, Xian-Fu Zhang, Mingna Feng, Siwen Zhao, Jing Zhang

PII: S0143-7208(18)32412-4

DOI: https://doi.org/10.1016/j.dyepig.2019.01.019

Reference: DYPI 7292

To appear in: *Dyes and Pigments*

Received Date: 1 November 2018

Revised Date: 6 January 2019

Accepted Date: 14 January 2019

Please cite this article as: Hu W, Lin Y, Zhang X-F, Feng M, Zhao S, Zhang J, Heavy-atom-free charge transfer photosensitizers: Tuning the efficiency of BODIPY in singlet oxygen generation via intramolecular electron donor-acceptor interaction, *Dyes and Pigments* (2019), doi: https://doi.org/10.1016/j.dyepig.2019.01.019.

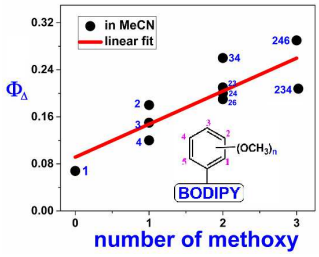

Singlet oxygen formation yield of $(CH_3O)_n$-phenyl-BODIPY donor-acceptor conjugate is proportional to the number of methoxy group.

Heavy-atom-free charge transfer photosensitizers: Tuning the efficiency of BODIPY in singlet oxygen generation via intramolecular electron donor-acceptor interaction

Wenbin Hu[a], Yanhe Lin[a], Xian-Fu Zhang[b,*], Mingna Feng[a], Siwen Zhao[a], Jing Zhang[a]

[a] College of Chemical Engineering, Hebei Normal University of Science and Technology, Qinhuangdao, Hebei Province, China, 066004

[b] MPC Technologies, Hamilton, Ontario, Canada L8S 3H4

*Corresponding author

E-mail addresses: zhangxianfu@tsinghua.org.cn, zhangxf111@hotmail.com

Abstract

To test the tunability of charge transfer (CT)-based BODIPY photosensitizers in generating singlet oxygen ($^1\Delta_g$), twelve *meso*-phenyl-BODIPY (donor-acceptor) type compounds have been synthesized and fully characterized, in which the phenyl moiety is modified with respective 0, 1, 2 and 3 methoxy groups to increase its electron-donating ability. The UV-Vis absorption spectra, fluorescence emission spectra, fluorescence quantum yield, fluorescence lifetime, excited triplet state formation, and singlet oxygen formation properties are measured. DFT quantum chemical computation is also carried out to explain the experiments. The occurrence of intra-molecular CT is confirmed by UV-Vis absorption, fluorescence properties and quantum chemical computation. The triplet excited state formation is evidenced by laser flash photolysis technique. The quantitative photosensitized singlet oxygen formation is demonstrated by DPBF (diphenylisobenzofuran) chemical trapping method.

This type of BODIPY CT photosensitizers show good tunability in generating singlet oxygen ($^1\Delta_g$). When the number of methoxy group on the donor is increased (so that CT is enhanced), the efficiency of singlet oxygen generation becomes higher from 0.070 to 0.30. When solvent polarity is increased (CT is also enhanced), the efficiency of singlet oxygen generation is also increased significantly. The increase in singlet oxygen generation is accompanied by the decrease in fluorescence quantum yield and fluorescence lifetime values. These facts show that a higher CT efficiency in a simple phenyl-BODIPY donor-acceptor conjugate can lead to significant higher quantum yield of singlet oxygen generation. These results are useful in designing novel CT-based heavy-atom-free photosensitizers for photodynamic therapy of tumor.

Keywords: Charge transfer photosensitizer; singlet oxygen; BODIPY; photodynamic therapy

1. Introduction

Photosensitizers (PSs) that generate singlet oxygen ($^1\Delta_g$) are the key of photodynamic therapy of tumor (PDT) [1-5]. PDT has great potential for the treatment of various cancers [6,7] and drug-resistant microbes [8,9], due to its many advantages over the traditional chemotherapy [10-12], including higher precision of the targets, lower systemic damage, non-invasion, reusable and controllable characteristics. PDT relies on three basic elements: PS, light, and molecular oxygen. A traditional PS molecule absorbs specific light and becomes an excited singlet state S_1 ($S_0 + hv \rightarrow S_1$), S_1 then transforms to a triplet excited state T_1 with slightly lower energy ($S_1 \rightarrow T_1$), T_1 then gives its energy to a surrounding oxygen molecule and results in the formation of singlet oxygen $^1O_2$ [13,14]: $T_1 + O_2 \rightarrow S_0 + {}^1O_2(^1\Delta_g)$. Singlet oxygen $^1O_2$ ($^1\Delta_g$) is considered to be the main reactive oxygen species (ROS) for the tissue ablation in PDT [15,16].

Charge transfer (CT)-based photosensitizers (CTPSs) are new members of PS family [17-21]. A traditional PS generates T_1 from its S_1 state via the spin flipping of the electron in the molecular LUMO,

S_1:HOMO(↑)LUMO(↓) **or** HOMO(↓)LUMO(↑) ⟶ **T_1**: HOMO(↑)LUMO(↑) **or** HOMO(↓)LUMO(↓).

However, this type of electron spin reversing in S_1 of some compounds is not efficient. 4,4-difluoro-4-bora-3a,4a-diaza-*s*-indacene (BODIPY) derivatives are such examples. Nonhalogenated BODIPYs show very low T_1 formation quantum yield because they are highly fluorescence emissive. In recent years, BODIPYs have been proposed as PSs for PDT due to their high molar extinction coefficient, good photochemical stability, chemically robustness and good solubility in organic solvents [22,23]. To this aim heavy atom effect have been attached to a BODIPY to make them efficiently generate T_1 [24,25]. In recent studies, however, PCT (Photoinduced CT) or PET (Photoinduced electron transfer) are also found to be very efficient for causing T_1 and singlet oxygen formation, especially for BODIPY dyes [26-29]. The PCT/PET-based PSs are advantageous because they are halogen-free and easily tailored to act as activable PSs. A donor-acceptor (D-A) type molecular structure is a prerequisite for

this type of PSs. The mechanism of T_1 generation for these PSs is: S_1 generates charge separated state (CSS) via PET/PCT:

$$\text{D-BODIPY}(S_1) \rightarrow D^{\delta+}\text{-BODIPY}^{\delta-}\ (0<\delta\leq 1),$$

and then charge recombination of CSS produces T_1:

$$D^{\delta+}\text{-BODIPY}^{\delta-} \rightarrow \text{D-BODIPY}(T_1),$$

this is possible because S_1 energy > CSS energy > T_1 energy. The reported PET/PCT-based BODIPY PSs are mainly *meso*-aryl-BODIPY conjugates, where the aryl moiety is a relatively large electron donor, such as pyrene, anthracene, and naphthalene [27-29].

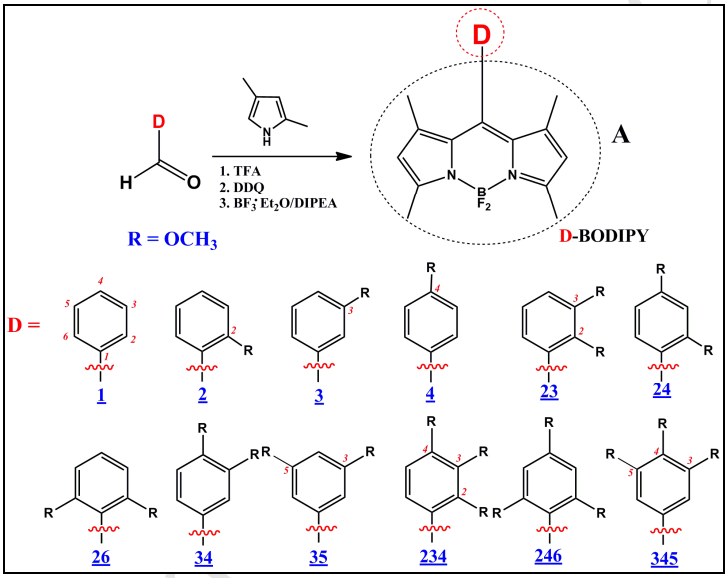

Fig. 1. Structures of the methoxy-functionalized sensitizers

In order to make the PCT/PET-based BODIPY PSs easier use *in vivo*, we show in this report that even the *meso*-phenyl-BODIPY can be easily modified to remarkably increase the efficiency of BODIPY in T_1 and singlet oxygen formation. We therefore have synthesized a library of one to three *meso*-methoxys modified phenyl-BODIPY conjugates. The increase in the number of methoxy on the phenyl makes the moiety a better electron donor and enhances PCT/PET from the phenyl to BODIPY, which significantly promotes the generation of T_1. By changing the number and position of methoxys on the phenyl, we expect to finely tune the singlet oxygen generation efficiency. Fig. 1 shows the structures of the studied BODIPYs. BODIPY **2, 3** and **4**

contain one methoxy group, BODIPY **23**, **24**, **26**, **34** and **35** contain two methoxys, while BODIPY **234**, **345** and **246** contain three methoxys on the phenyl. The starting materials are cheap and commercially available, while the preparation procedure for the compounds is simple and only involves one pot reaction.

2. Experimental section

2.1. Reagents and Apparatus

All chemicals were purchased from Sigma-Aldrich, Acros Organics, Merck or Fluka at the highest commercial grade and were used without further purification. All solvents were dried and redistilled before use. Dry solvents were prepared with standard methods [30,31]. Merck 60 F254 silica gel precoated sheets (0.2 mm thick) were used for analytical thin-layer chromatography (TLC). Silica gel (200-400mesh, Merck) was used for flash column chromatography. ^{1}H and ^{13}C NMR spectra were recorded with a Bruker dmx NMR spectrometer (600 MHz for ^{1}H and 75 MHz for ^{13}C). The spectra were recorded in $CDCl_3$. ^{1}H NMR chemical shifts are reported in parts per million relative to tetramethylsilane (δ = 0.00 ppm), using the residual solvent signal as the internal reference. ^{13}C NMR chemical shifts are reported in ppm with $CDCl_3$ (δ = 77.67 ppm) as the internal standard. Carbon spectra were broad band decoupled and calibrated on the particular solvent signal. Chemical shift multiplicities were indicated by s (singlet), d (doublet), t (triplet), q (quartet), m (multiplet) and br (broad). The unit of the coupling constant is Herz (Hz). Mass spectra were registered by atmospheric pressure chemical injection (APCI) in a LTQ Orbitrap XL TOF spectrometer.

2.2. Synthesis

General Procedure for the Synthesis of BODIPYs: The synthetic procedure for BODIPY **(Fig. 1)** is analogous to that described in ref [27-29]. An appropriate aldehyde (1.0 mmol) and 2,4-dimethylpyrrole (0.200g, 2.1 mmol) were added to absolute dichloromethane (20 mL). The color of the solution was turned into red after

the addition of one drop of trifluoroacetic acid. The reaction mixture was then quickly stirred at room temperature for 18 hours. 2,3-dicyano-5,6-dichlorobenzoquinone (0.227g, 1.0 mmol) was added, and stirring was continued for 120 min. *N*,*N*-Diisopropylethylamine (5ml) and boron trifluoride etherate (10ml) were added to the solution sequentially. After stirring for 12 hours, the reaction mixture was washed with water. Organic layer was dried with anhydrous $MgSO_4$, filtered, and evaporated under reduced pressure. The crude product was purified by silica gel column chromatography using 20 % dichloromethane in n-hexane as mobile phase. The brightly fluorescent fraction containing the product was collected then the solvent was removed under reduced pressure.

5,5-difluoro-10-(2-methoxyphenyl)-1,3,7,9-tetramethyl-5H-dipyrrolo[1,2-c:2',1'-f][1,3,2]diazaborinin-4-ium-5-uide (**2**). Yield: 21%. Orange crystals. ^{1}H NMR ($CDCl_3$, 600 MHz): δ 7.44 (t, 1H, J=6.66), 7.14 (d, 1H, J=7.40), 7.08 (t, 1H, J=7.38), 6.99 (d, 1H, J=8.34), 5.96 (s, 2H), 3.77 (s, 3H), 2.55 (s, 6H), 1.43 (s, 6H). ^{13}C NMR ($CDCl_3$, 150 MHz): δ 156.41, 154.92, 142.60, 138.96, 131.56, 130.63, 129.52, 123.81, 121.51, 120.85, 111.14, 55.62, 14.61, 13.84. HRMS (APCI) *m/z*: 335.1714 $[M-F]^+$ ($[M-F]^+$ calcd. 335.1731).

Characterization data for eleven other compounds are given in supporting information.

2.3. Photophysical characterization

Details of the photophysical properties of BODIPYs, including absorption, fluorescence spectra, singlet oxygen and fluorescence quantum yields, and fluorescence lifetime are given in our previous publication [28-29].

2.3.1. Absorption Measurements

Ground-state UV-visible absorption of BODIPYs were recorded on a Vary 8454 spectrometer from Agilent Technologies in a quartz cell of 1 cm path length at 20.0 ± 0.5 °C.

2.3.2. Fluorescence Measurements

Fluorescence excitation and emission spectra, fluorescence quantum yields, the fluorescence and excited singlet state lifetimes were acquired on a FLS 920 Fluorescence Spectrometer from Edinburgh Instruments at 20 ºC. 1 cm pathlength cuvettes were used, and the slit width was 2.5 nm for both excitation and emission. All spectra were corrected for the sensitivity of the photomultiplier tube. All measurements, both absorbance and emission, were acquired within 2 h of solution preparation at room temperature (20-25 ºC),

(1). Fluorescence quantum yield (Φ_f) of the BODIPYs was determined by the comparative method using equation (1).

$$\Phi_f = \Phi_f^0 \cdot \frac{F_s}{F_0} \cdot \frac{A_0}{A_s} \frac{n_s^2}{n_0^2} \qquad (1)$$

F is the area under the fluorescence emission curve, and the areas of the emission spectra were integrated in the range of 480 - 700 nm. A represents the optical density at which the sample was excited. The refractive indices (n) of the solvents were employed in calculating the fluorescence quantum yields in different solvents. The subscript 0 stands for a reference compound, and s represents samples. Fluorescein in 0.1 M NaOH was used as the reference (Φ_f^0= 0.92) [32]. The excitation wavelength is 475 nm. The absorbance of the sample and reference solutions at the excitation wavelength ranged between 0.08 and 0.10. All solutions were air saturated for Φ_f measurements.

(2). Fluorescence lifetime was measured by Edinburgh FLS920 spectrophotometer via the time-correlated single photon counting (TCSPC) method with excitation at 509 nm by a diode laser (50 ps fwhm). The emission was monitored at the wavelength of emission maximum. The lifetime values were computed by the F900 software supplied by Edinburgh Instruments Ltd.

2.3.3. Singlet oxygen quantum yield

The quantum yield of singlet oxygen production was determined by the chemical trapping method using diphenylisobenzofuran (DPBF). The absorbance of the studied

BODIPYs was adjusted around 1.0 at 509 nm (irradiation wavelength) in 1 cm path length quartz cells (2 mL). The absorbance of DPBF was adjusted around 1.0 at 410 nm in order to avoid BODIPY aggregation. Singlet oxygen causes a remarkable degradation of DPBF at 410 nm, where the DPBF absorbance decrease was measured at fixed time intervals, as defined for each experiment. The quantum yields of singlet oxygen generation were calculated by comparing with that of the reference compound 8-methylthio-2,6-diiodoBODIPY according to Equation (2)

$$\Phi_{\Delta} = \Phi_{\Delta}^{ref} \frac{k}{k^{ref}} \frac{I_a^{ref}}{I_a} \quad (2)$$

Where Φ_{Δ}^{ref} is the singlet oxygen quantum yield for the standard (8-methylthio-2,6-diiodoBODIPY, Φ_{Δ}^{R}=0.85, practically independent of the solvent) for excitation at 505 nm), k and k_{ref} represent the DPBF photobleaching rate constants in the presence of the respective samples and standard, respectively, and I_a and I_a^{ref} stand for the number of photons absorbed by the sensitizer and the standard at the irradiation wavelength of 509 nm, respectively. Their ratio can be obtained by the following equation:

$$\frac{I_a^{ref}}{I_a} = \frac{1-10^{-A_{ref}}}{1-10^{-A}} \quad (3)$$

In which, A and A_{ref} is the absorbance of a BODIPY and the reference compound 8-methylthio-2,6-diiodoBODIPY at excitation wavelength 505 nm, respectively.

2.4. Computational simulation

The calculations were carried out using density functional theory (DFT) method as implemented in the Gaussian 09 package. The B3LYP exchange-correlation functional was chosen together with a 6-311G basis set for structural optimization. The solvent effect was modeled using the Polarizable Continuum Model (CPCM) method. In all the cases frequency analysis was made after geometry optimization to ensure the convergence to an energy minimum.

3. Results and discussion

A *meso*-$(OCH_3)_x$phenyl-BODIPY (x=1, 2, 3) forms an intro-molecular donor-acceptor (D-A) entity which act as the PCT-based photosensitizer in this study. *meso*-(methoxy)$_x$phenyl is the donor moiety, while the BODIPY is the acceptor. Keeping the BODIPY unit unchanged, adding more methoxys onto the phenyl at different positions, the charge transfer intensity from **D** to **A** is then affected by three factors: the number of methoxys, the position of the methoxys, and solvent polarity. By changing any one of the three factors, we can tune the efficiency of singlet oxygen formation if the D-A entity is really a CT-based photosensitizer. To this purpose, twelve *meso*-aryl BODIPYs have been synthesized by a facile three-step one-pot procedure (Fig. 1) [28-29]. These BODIPYs have been structurally identified by ^{1}H NMR, ^{13}C NMR, HRMS and UV-Vis absorption spectra. All the spectrum results are consistent with the desired structures. These NMR and HRMS spectra are presented in supplementary information.

Due to the presence of methoxy and the phenyl groups, these BODIPYs are all well soluble in organic solvents, such as *n*-hexane, benzene, toluene, DCM, chloroform, THF, ethyl acetate, acetone, ethanol, methanol, acetonitrile, DMF and DMSO. Seven solvents ranging from nonpolar, low polar to high polar ones (n-hexane, ethyl acetate, THF, pinacolone, acetone, methanol and acetonitrile) have been used to measure their photophysical properties and singlet oxygen generation ability.

3.1. Singlet oxygen formation tuned by methoxy and solvent polarity

The singlet oxygen formed by the BODIPY photosensitization was identified by chemical trapping method using 1,3-diphenylisobenzofuran (DPBF). DPBF is a well known specific chemical trapper of singlet oxygen ($^1\Delta_g$) [33]. As shown in Fig. 2, with light irradiation at 510 nm in air saturated acetonitrile (at which the light is absorbed only by the BODIPY PS) DPBF absorption (peak at 410 nm) decreases with time while the absorption of the BODIPY shows no change. In the absence of any one

of oxygen (purged by bubbling argon), light irradiation, or a BODIPY PS, the absorbance decrease of DPBF at 410 nm did not occur. These results mean that the singlet oxygen formation is indeed due to photosensitization of the BODIPY.

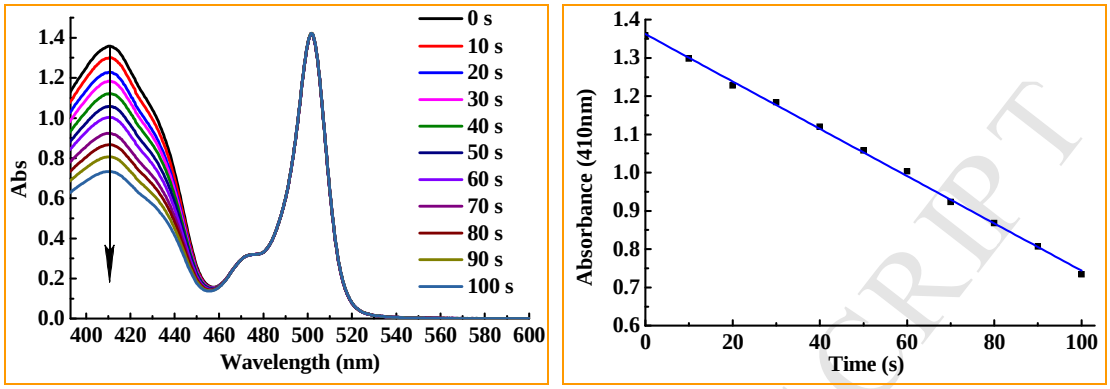

Fig. 2. Left: Evolution of DPBF (60 µmol/L) absorption spectra in air saturated acetonitrile containing BODIPY **246** (20 µmol/L) with light excitation at 510 nm. **Right**: Absorbance decrease of DPBF at 410 nm with time (data extracted from spectra of Fig. 2 left).

The quantum yield of singlet-oxygen formation (Φ_Δ) was obtained by measuring the photooxidation kinetics of DPBF. The DPBF absorbance at 410 nm is plotted against time (Fig. 2 right). A good linear relation between them indicates that the reaction kinetics is zero order: $c(t) = c(0) - k \cdot t$, in which k is the reaction rate constant, t is time, and c(t) is the concentration of DPBF at time t. Singlet oxygen quantum yields (Φ_Δ) of the studied BODIPYs were calculated according to the literature [34,35]. The reference compound 8-methylthio-2,6-diiodoBODIPY has a singlet oxygen quantum yield of 0.80 under the conditions of the study in all solvents [36].

Table 1 shows the Φ_Δ values together with other photophysical parameters (also see Table S1 of supporting information). Compared to BODIPY **1** that contains an unsubstituted phenyl, the methoxy substitution leads to higher Φ_Δ values. Fig. 3 plots Φ_Δ against ε (solvent dielectric constant to represent polarity) and **n** (number of methoxys), respectively. It shows that Φ_Δ value increases with the increase in the number of methoxy groups on the phenyl moiety, and this increase is more effective in more polar solvent. The position of methoxys also affects Φ_Δ values, but in a complicated way as shown in Fig. 3 bottom. These BODIPYs exhibit very significant

solvent effect: a higher Φ_Δ value is observed in a more polar solvent. The data in methanol for all compounds show deviation from the trend, likely because the strong H-bonding O–H • • • F. In order to explain these results, UV-vis absorption spectra, fluorescence emission spectra, fluorescence lifetimes, and transient absorption properties were measured.

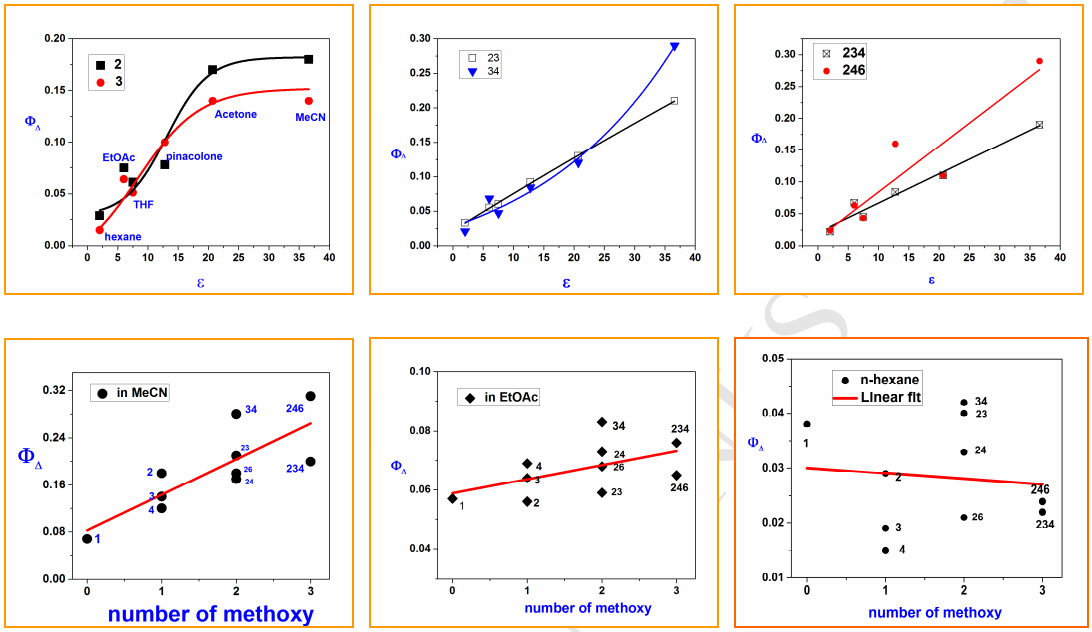

Fig. 3. Top: solvent polarity (ε) effect on Φ_Δ. Bottom: the influence of **n** (number of methoxy on the phenyl) on Φ_Δ (next to each data point is the compound number), the red line is the linear fitting results.

Table 1. Photophysical properties of the BODIPY PSs in different solvents**

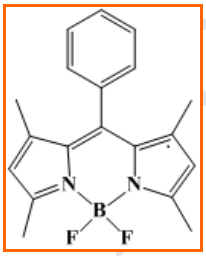

1

Solvent	ε	Φ_f	Φ_Δ	λ_{max}^{abs} (nm)	λ_{max}^{em} (nm)	$\Delta\lambda$ (nm)	τ_f (ns)	χ^2
CH_3CN	36.6	0.52	0.068	497	508	11	3.81	1.00
Acetone	20.7	0.46	0.050	498	509	11	3.65	1.24
Pinacolone	12.8	0.55	0.11	499	511	12	3.39	1.18
EtOAc	6.02	0.58	0.057	498	510	12	3.98	1.18
THF	7.52	0.56	0.033	500	512	12	3.73	1.12
n-hexane	2.02	0.56	0.038	501	511	10	3.37	1.27
MeOH	33	0.58	0.031	498	510	12	3.9	1.22

** Φ_f: fluorescence quantum yield, Φ_Δ: quantum yield for singlet oxygen formation, λ_{max}^{abs}: UV−vis absorption maximum, λ_{max}^{em}: fluorescence emission maximum, $\Delta\lambda$: the Stokes shift, τ_f: fluorescence lifetime, χ^2: chi squared value for fluorescence decay that obtaining τ_f.

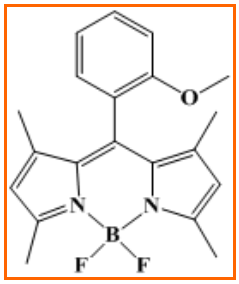

2

Solvent	ε	Φ_f	Φ_Δ	λ_{abs} (nm)	λ_{em} (nm)	$\Delta\lambda$ (nm)	τ_1 (ns)	χ^2
CH_3CN	36.6	0.57	0.18	499	512	13	-	-
Acetone	20.7	0.78	0.17	501	513	12	-	-
Pinacolone	12.8	0.74	0.078	502	514	12	-	-
EtOAc	6.02	0.76	0.057	502	514	12	-	-
THF	7.52	0.87	0.061	503	516	13	6.42	1.19
n-hexane	2.02	0.98	0.029	504	516	12	5.78	1.11
MeOH	33	0.69	0.021	500	514	14		

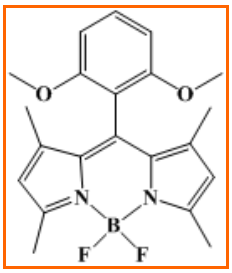

26

Solvent	ε	Φ_f	Φ_Δ	λ_{abs} (nm)	λ_{em} (nm)	$\Delta\lambda$ (nm)	τ_1 (ns)	τ_2 (ns)	χ^2
CH_3CN	36.6	0.54	0.18	500	513	13	-	-	-
Acetone	20.7	0.72	0.082	503	516	13	-	-	-
Pinacolone	12.8	0.64	0.081	505	520	15	-	-	-
EtOAc	6.02	0.47	0.073	504	520	16	-	-	-
THF	7.52	0.64	0.051	506	520	14	5.77	1.38(.12)	1.08
n-hexane	2.02	0.71	0.040	507	519	12	6.26	-	1.09
MeOH	33	0.58	0.036	503	518	15	-	--	

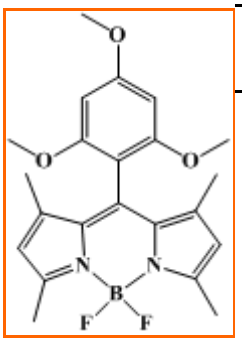

246

solvent	ε	Φ_f	Φ_Δ	λ_{abs} (nm)	λ_{em} (nm)	$\Delta\lambda$ (nm)	τ_1 (ns)	τ_2 (ns)	χ^2
CH_3CN	36.6	0.55	0.31	501	513	12	-	-	-
Acetone	20.7	0.80	0.11	503	515	12	-	-	-
Pinacolone	12.8	0.69	0.16	505	517	12	-	-	-
EtOAc	6.02	0.64	0.063	503	511	8	-	-	-
THF	7.52	0.78	0.059	506	517	11	5.70	1.35(.05)	1.14
n-hexane	2.02	0.95	0.024	505	520	15	6.35	-	1.10
MeOH	33	0.68	0.074	503	515	12	-	-	-

3.2. UV-Vis absorption spectra and intra-molecular donor-acceptor charge transfer

The UV/vis absorption and fluorescence properties of these BODIPYs in different solvents are also included in Table 1 (and Table S1 of supporting information). Fig. 4 shows the spectra of compound **2**, **26** and **246**. Most compounds display the typical UV-Vis absorption spectra of BODIPY type (supporting information):[37] a main band at about 500 nm with a shoulder at ca. 475 nm, and a weak band at ca. 360 nm. For compound **26** and **246**, however, an additional weak band occurs at ca. 525 nm. This new band is red shifted relative to the usual main

band, and the intensity of the new band is sensitive to the solvent polarity. These characters suggest the new bands are due to CT (charge transfer) absorption. The CT absorption occurs only for compound **26** and **246**, likely because the two methoxys at position 2 and 6 of the phenyl are the closest to the BODIPY unit and better facilitates charge transfer compared to other methoxys.

As is evident from Table 1, the main absorption band for each compound is centered between 497 and 507 nm and the peak maximum is not sensitive to either solvent polarity or the number and position of methoxy group, because the methoxy is not directly attached to the BODIPY chromophore but to the phenyl (which is nearly orthogonal to the BODIPY).

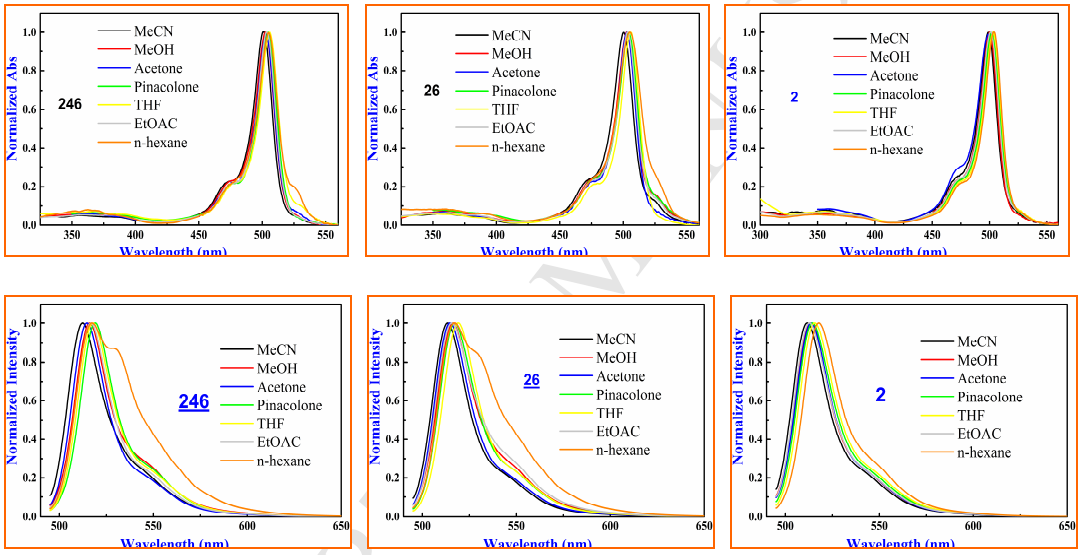

Fig. 4. Top: Normalized UV-Vis absorption spectra of **2**, **26**, and **246** in different solvents. **Bottom**: Normalized fluorescence emission spectra of **2**, **26**, and **246** in different solvents (excitation at 475 nm, concentration ca. 5 μM).

3.3. Fluorescence Studies

The presence of the methoxys cause the change in fluorescence spectrum, fluorescence quantum yield, and lifetime reflects the intensity of photoinduced charge transfer from the donor to the acceptor. Fig. 4 shows the fluorescence spectra of the BODIPY donor-acceptor conjugates in different solvents. These compounds exhibit fluorescence in the range 500–550 nm, which is the typical emission characteristics of

BODIPY fluorophores [38]. For compound **26** and **246**, however, a new band occurs at about 530 nm. This red shifted and weak emission shows the characteristics of CT emission. The associated photophysical processes are given below.

Light absorption: $D\text{-}A(S_0) + \mathbf{hv} \rightarrow D\text{-}A(S_1)$, (i)

Fluorescence: $D\text{-}A(S_1) \rightarrow \mathbf{hv'} + D\text{-}A(S_0)$, (ii)

Charge transfer: $D\text{-}A(S_1) \rightarrow D^{\delta+}\text{-}A^{\delta-}$, (iii)

CT emission: $D^{\delta+}\text{-}A^{\delta-} \rightarrow \mathbf{hv''} + D\text{-}A(S_0)$, (iv)

Charge recombination: $D^{\delta+}\text{-}A^{\delta-} \rightarrow \mathbf{heat} + D\text{-}A(S_0)$, (v)

Since CT state $D^{\delta+}\text{-}A^{\delta-}$ easily undergoes fast reverse thermal charge transfer in polar solvents to form ground state (process v), CT emission is observed only in hexane. The CT emission band occurs only for compound **26** and **246**, because the two methoxys at position 2 and 6 of the phenyl are closer to the BODIPY unit than other methoxys, which better facilitates charge transfer.

Except for that of **26** and **246** in hexane, the fluorescence emission spectrum of each BODIPY is the mirror image of the corresponding main absorption band, which implies that the emission is due to S_1 decay of the BODIPY unit [39]. The Stoke shifts of the BODIPYs are in the range 10-17 nm. The small Stoke shift is typical for BODIPY compounds, indicating that the S_1 of BODIPY unit has similar nuclear configurations to its ground state. All these BODIPYs share the same fluorophore and therefore exhibit very similar emission shape in different solvents except hexane. Increasing the solvent polarity for each compound causes only a slight shift in the emission maximum to longer wavelength (~2-6 nm) while the shape of emission spectra is not changed (except **26** and **246** in hexane). These results show that the remarkable solvent dependence of Φ_Δ values does not result from the interaction between the solvent and the BODIPY (either S_0 or S_1 state).

The fluorescence quantum yield (Φ_f) values of each BODIPY in different solvents are also listed in Table 1 (and Table S1 of supporting information). Fig. 5 shows how the substitution pattern and solvent polarity (represented by ε) affect the Φ_f value of a BODIPY conjugate. It is known that

$$\Phi_f = k_f/(k_f+k_{isc}+k_{ic}+k_{CT}), \quad (4)$$

in which k_f is the fluorescence rate constant, k_{isc} is the intersystem crossing rate constant for T_1 formation, k_{ic} is the internal conversion rate constant for heat releasing, and k_{CT} is the charge transfer rate constant.

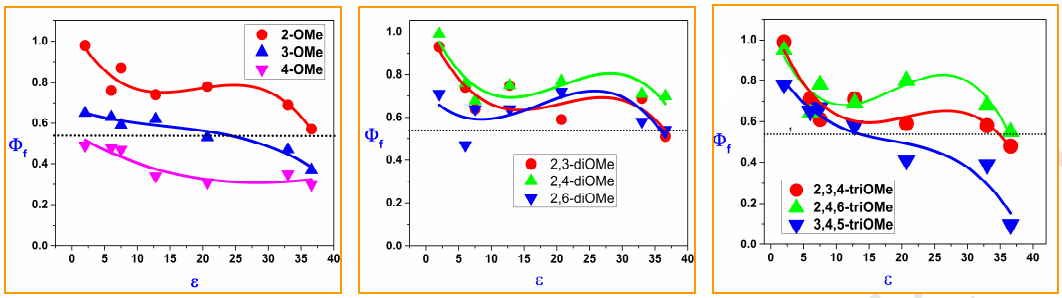

Fig. 5. Solvent polarity (represented by dielectric constant ε) effect on Φ_f. **Left**: mono substituted BODIPY **2**, **3,** and **4**. **Middle**: di substituted BODIPY **23**, **24**, and **26**. **Right**: tri substituted BODIPY **234**, **246**, and **345**. The dashed line in each plot is for unsubstituted BODIPY **1**.

Several conclusions can be drawn from Fig. 5 as following. The Φ_f value of each compound shows clear decrease trends with the increase in solvent polarity except the slight positive deviation of a few solvent. This decrease trend is consistent with the effect of solvent polarity on photoinduced charge transfer or electron transfer. Since k_{CT} of PCT/PET becomes larger in more polar solvent, so intramolecular PCT/PET partially quenches emission process and leads to a lower Φ_f value according to eq. (4). This change is opposite to the effect of solvent polarity on Φ_Δ value, which implies that singlet oxygen production is positively correlated to the intensity of PCT or PET. Since singlet oxygen originates from the T_1 of a photosensitizer, we conclude that T_1 formation is positively correlated to PCT or PET.

Triplet formation from CT state: $D^{\delta+}\text{-}A^{\delta-} \rightarrow \text{D-A}(T_1)$, (vi)

$^1O_2$ generation from T_1: $\text{D-A}(T_1) + O_2 \rightarrow \text{D-A}(S_0) + {}^1O_2$. (vii)

Based on the processes (i) to (vii), we can easily understand Fig. 3 which shows how solvent polarity and methoxy number affect Φ_Δ value. Higher solvent polarity enhances charge transfer process (iii) and leads to more CT state formation, then more CT state favors process (vi) and causes more T_1 formation, which further gives more singlet oxygen through process (vii). The increase in the number of methoxy on the

phenyl enhances the electron donating ability of the phenyl moiety, which favors better charge transfer, and then leads to higher Φ_Δ value. Φ_Δ value is mainly determined by k_{CT} value for these BODIPYs, since k_{isc} is negligible for BODIPYs and not affected by the number and position of methoxy group.

Fig. 5 also indicates the effect of methoxy position on Φ_f. Φ_f value is influenced by both k_{ic} and k_{CT} for these OCH_3 modified BODIPYs, since the position of methoxy changes k_{ic}, while both the number and position of methoxys alter k_{CT}. For mono OCH_3 compounds, compared **2** shows higher Φ_f than **1** (the dashed line) in each solvent, but compound **4** always exhibits lower Φ_f than **1** in each solvent. This is due to both steric and electronic effect. In addition to its electronic effect, the OCH_3 group in compound **2** obstructs the rotation of the phenyl, which reduces the k_{ic} value and increases Φ_f. Therefore 2'-OCH_3 is dominated by steric effect over its electronic effect. The OCH_3 group in compound **4**, however, has no steric effect but exhibits only electron donating effect which increases k_{CT} and decreases Φ_f. The OCH_3 group in compound **3** is farther away than that in compound **2** but closer than that in compound **4** from the BODIPY unit, and therefore it displays weaker steric effect than that of compound **2** but stronger steric effect than that of compound **4**. This explains the Φ_f ranking **2**>**3**>**4** in each solvent. Di- and tri-methoxy substituted BODIPYs are some complicated due to the mutual influence of steric and electronic effect of each OCH_3 group at different positions. Nevertheless, the Φ_f ranking of trisubstituted BODIPYs is **246**>**234**>**345** in each solvent, because **246** contains two methoxys at position *2* and *6* that both show strong steric effect, **234** contains one 2-methoxy, while **345** contains none.

The fluorescence lifetime of **2, 26**, and **246** in hexane and THF were measured to confirm the presence of PCT in polar solvents. Fig. 6 shows the emission decay curves of these BODIPYs. For **26** and **246**, the decay in polar THF is faster than that in non polar n-hexane. For compound **2**, the solvent effect on the emission decay is not significant. In hexane, the fluorescence decays can be described by a single-exponential fit, and the calculated lifetime is 5.78, 6.26, and 6.35 ns for **2**, **26**, and **246** respectively. In THF, however, the decays of BODIPY **26** and **246** become

biexponential, the lifetime for **26** is 1.38 (12%) and 5.77 ns (88%), and the lifetime for **246** is 1.37 (5%) and 5.70 ns (95%). Comparing the lifetime value of the short-lived component in THF with the lifetime in n-hexane, we see a very significant decrease from 6.26 to 1.38 ns for **26**, and from 6.35 ns to 1.37 ns for **246**. This large decrease in more polar solvent supports the presence of intramolecular PCT/PET. By using equation $k_{CT} = 1/\tau_f - 1/\tau_f^0$, the rate constant of PCT/PET (k_{CT}) in THF can be calculated as 0.564×10^9 and 0.572×10^9 s^{-1} for **26** and **246**, respectively. In the mean time, the emission rate constant ($k_f = \Phi_f/\tau_f$ in hexane) can be calculated as 0.11×10^9 and 0.15×10^9 s^{-1} for **26** and **246**, respectively. So k_{CT} is much larger than k_f in THF, i.e. PCT becomes the predominant process of S_1 decay in THF.

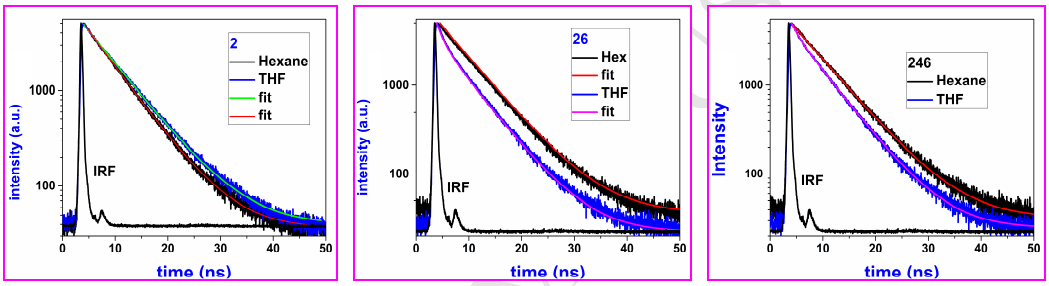

Fig. 6. The emission decay curves of the BODIPY **2**, **26**, and **246** with excitation at 405 nm (50 ps pulsed laser).

3.4. CT from quantum chemical calculations

The molecular geometry of the D-A conjugates is optimized either by DFT (for ground state S_0) or TD DFT (for excited state S_1) at the B3LYP 6-311g level. The HOMO and LUMO of a compound are then obtained from the calculated geometry. The HOMO and LUMO electron density distribution between the donor and acceptor units provides the evidence of PCT occurrence within the D-A type conjugated molecules. In Fig. 7, we compare the electron density change of frontier molecular orbitals of compound **2**, **24**, and **246** upon the change of solvent and/or photo excitation.

For compound **246** (Fig. 7), in either vacuum or non polar solvent hexane, the HOMO and LUMO of both S_0 and S_1 are mainly located on the BODIPY unit (Fig. 7 Top), indicating that ground state CT or photoinduced CT must be weak in vacuum or

non polar solvent hexane. In acetonitrile (ACN), however, the HOMO of S_0 is located on both BODIPY and the phenyl unit, but the LUMO of S_0 is located only on BODIPY unit, indicating that ground state CT can occur. This result shows the strong effect of solvent polarity. On the other hand, the HOMO of S_1 of **246** in acetonitrile is located only on the phenyl unit, but the LUMO of S_1 is located only on BODIPY unit, suggesting that photoinduced electron transfer (complete charge transfer) occurs from the trimethoxy phenyl unit to the BODIPY moiety, which causes the fluorescence quenching and lowers Φ_f and τ_f values. This result shows the strong effect of photoexcitation on PCT/PET.

For compound **24** (Fig. 7 bottom left), photoinduced CT occurs only for S_1 state in acetonitrile, because the HOMO of S_1 is located on both BODIPY and the phenyl unit, while the LUMO of S_1 is located only on BODIPY unit. In other cases, CT or PCT is not significant since both HOMO and LUMO are mainly on the BODIPY unit.

For compound **2** (Fig. 7 bottom right), no significant CT or PCT can occur since both HOMO and LUMO are always mainly on the BODIPY unit. Based on Fig. 7, it is obvious that the intensity of CT or PCT is ranked by **246**>**24**>>**2**, which confirms that the number of methoxy group shows large effect on CT and PCT.

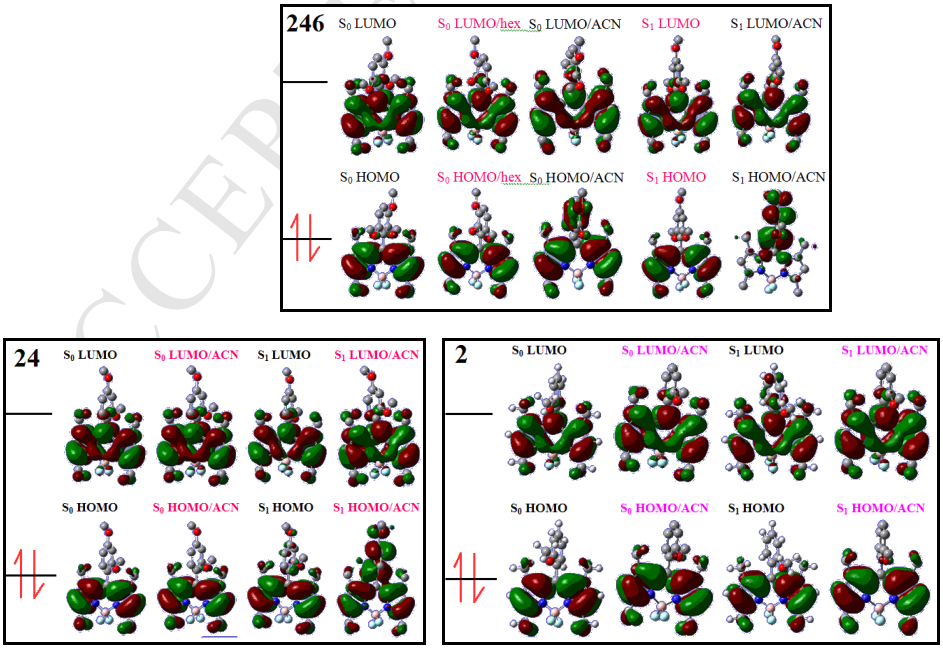

Fig. 7. The HOMO/LUMO of S_0 and S_1 state of compound **2**, **24**, and **246** calculated by DFT method using B3LYP exchange-correlation functional together with a 6-311G basis set. The solvent effect was modeled using the Polarizable Continuum Model (CPCM) method.

ACN=CH_3CN, hex = n-hexane.

3.5. Triplet excited state identification

Nanosecond laser flash photolysis (LFP) was used to confirm the ability to form excited triplet state T_1 for the donor-BODIPY conjugate. Using **246** as an example, the BODIPY moiety is excited at 510 nm (4 ns pulsed laser with energy of 4 mJ) in nitrogen saturated CH_3CN solution. Fig. 8 shows the transient absorption spectra (TAS) and the triplet decay curves. The positive absorption bands were observed at 435 nm. No significant TAS signal was detected for compound **1**. The band shape and positions are similar to the reported triplet-triplet (T_1-T_n) absorption of other BODIPY analogues.[16, 17] The negative signal matches the images of ground state absorption spectra. From the spectra in Fig. 8, we can see that the decay of the positive signal is accompanied by the rise of negative signal (formation of S_0 state), during which an isobestic point exists. The decay lifetime of the positive signal is the same as that of the rise lifetime of the negative signal (Fig. 8 middle). Further more, the decay lifetime is 0.35 μs in air saturated CH_3CN for **246**, but it becomes much longer as 6.4 μs in N_2 saturated CH_3CN (Fig. 8 right). These results show that excited triplet state is indeed formed by the $(OMe)_3$-phenyl substituted BODIPY upon light excitation.

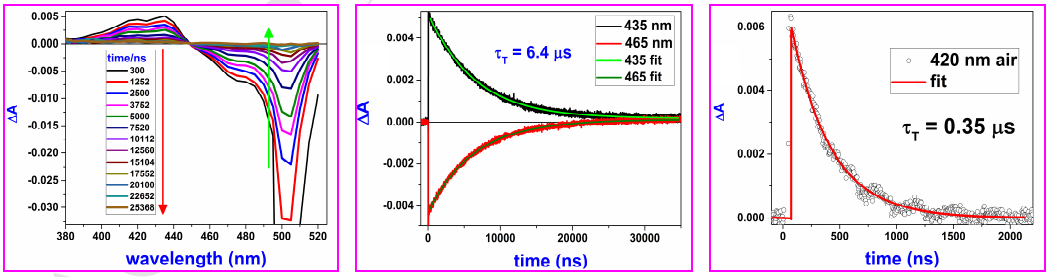

Fig. 8. Left: the transient absorption spectra of **246** (20 μM) in nitrogen saturated CH_3CN solution. **Middle**: the triplet decay curve of 435 nm and the ground state recovery at 465 nm in nitrogen saturated CH_3CN solution. **Right**: the triplet decay of 420 nm in air saturated CH_3CN solution. The BODIPY moiety is excited at 510 nm (4 ns pulsed laser with energy of 4 mJ).

4. Conclusions

We have synthesized and characterized twelve methoxy-phenyl-BODIPY donor-acceptor type new CT photosensitizers. Their absorption and fluorescence properties were measured in different solvents, from which intramolecular CT is evidenced and CT intensity is shown to depend on the number of methoxys on the phenyl. The singlet oxygen formation quantum yields in seven solvents were measured, from which it is established that Φ_Δ is positively related to CT intensity. The excited triplet state was identified by laser flash photolysis. The results show that Φ_Δ values are affected by the number and position of methoxys and solvent polarity. With the increase in solvent polarity, the Φ_f and τ_f values of these BODIPYs decrease but Φ_Δ values increase. In short, a simple phenyl-BODIPY can be tailed easily to donor-acceptor type halogen free CT photosensitizers. Further studies are in progress to improve the water solubility of these PET-based BODIPY photosensitizers and to develop their potential applications in destroying tumor cells through photodynamic therapy.

Acknowledgements

We gratefully acknowledge financial support by the Natural Science Foundation of Hebei Province (Contract B2016407084 and B2014407080), Youth Talent Program of Hebei High School (Contract BJ2017028), the Technology Foundation for Selected Overseas Chinese Scholar of Hebei Province (Contract C2015003046), Hebei Provincial Hundred Talents Plan (Contract E2013100005).

References

[1] M. H. Staegemann, S. Gräfe, B.Gitter, K. Achazi, E. Quaas, R. Haag and A. Wiehe, *Biomacromol.*, 2018; **19**: 222-38.

[2] M. Gorbe, A. M. Costero, F. Sancenón, R. Martínez-Máñez, R. Ballesteros-Cillero, L. E. Ochando, et al. Dyes and Pigments. 2019;160:198-207.

[3] J. P. Celli, B.Q. Spring, I. Rizvi, C. L. Evans, K.S. Samkoe, S. Verma, B. W.

Pogue and T. Hasan, *Chem. Rev.*, 2010; **110**: 2795-2838.

[4] F. Heinemann, J. Karges and G. Gasser, *Accounts. Chem. Res.*, 2017; **50**: 2727-36.

[5] J. Zhao, K. Xu, W. Yang, Chem. Soc. Rev. 2015;44(24):8904-39.

[6] D. E. Dolmans, D. Fukumura and R. K. Jain, *Nat. Rev. Cancer.*, 2003; **3**: 380-7.

[7] P. Agostinis, K. Berg, K. A. Cengel, T. H. Foster, A. W. Girotti, S. O. Gollnick, S. M. Hahn, M. R. Hamblin, A. Juzeniene, D. Kessel, M. Korbelik, J. Moan, P. Mroz, D. Nowis, J. Piette, B. C. Wilson and J. Golab, *CA Cancer J. Clin.*, 2011; **61**: 250-81.

[8] M. R. Hamblin and T. Hasan, *Photochem. Photobiol .Sci.*, 2004; **3**: 436-450.

[9] A. M. Durantini, D. A. Heredia, J. E. Durantini and E. N. Durantini, *Eur. J. Med. Chem.*, 2018; **144**: 651-61.

[10] J. F. Lovell, T. W. Liu, J. Chen and G. Zheng, *Chem. Rev.*, 2010; **110**: 2839-57.

[11] S. S. Lucky, K. C. Soo, Y. Zhang, *Chem Rev*., 2015; **115**: 1990-2042.

[12] L. Cheng, C. Wang, L. Feng, K. Yang and Z. Liu, *Chem. Rev.*, 2014; **114**: 10869-939.

[13] M. Triesscheijn, P. Baas, J. H. Schellens and F. A. Stewart, *Oncologist.*, 2006; **11**: 1034-44.

[14] K. Plaetzer, B. Krammer, J. Berlanda, F. Berr and T. Kiesslich, *Lasers Med. Sci.*, 2009; **24**: 259-68.

[15] K. P. Weishaupt, C. J. Gomer and T. J. Dougherty, *Cancer Res.*, 1976; **36**: 2326-9.

[16] B. W. Henderson and T. J. Dougherty, *Photochem. Photobiol.*, 1992; **55**: 145-57.

[17] J. Zhao, K. Chen, Y. Hou, Y. Che, L. Liu and D. Jia, *Org. Biomol. Chem.*, 2018; **16**: 3692-701.

[18] L. Y. Chung, L. Voon K. and H. B. Lee*, Photochem. Photobiol. Sci.*, 2018, Advance Article

[19] M. A. Filatov, S. Karuthedath, P. M. Polestshuk, S. Callaghan, K. J. Flanagan, T. Wiesner, F.c Laquai and M. O. Senge, *ChemPhotoChem*, 2018; **2**: 606-9.

[20] M. A. Filatov, S. Karuthedath, P. M. Polestshuk, S. Callaghan, K. J. Flanagan, M. Telitchko, T. Wiesner, F. Laquai and M. O. Senge, *Phys. Chem. Chem. Phys.*,

2018; **20**: 8016-22.

[21] X.-F. Zhang, X. Yang, B. Xu, *Phys. Chem. Chem. Phys.*, 2017;**19**: 24792-804.

[22] G. Ulrich, R. Ziessel and A. Harriman, *Angew. Chem. Int. Ed. Engl.*, 2008; **47**: 1184-201.

[23] A. Kamkaew, S. H. Lim, H. B. Lee, L. V. Kiew, L. Y. Chung and K. Burgess, *Chem Soc Rev.*, 2013; **42**: 77-88.

[24] J. Zhao, K. Xu, W. Yang, Z. Wang and F. Zhong, *Chem. Soc. Rev.*, 2015; **44**: 8904-39.

[25] T. Yogo, Y. Urano, Y. Ishitsuka, F. Maniwa and T. Nagano, *J. Am. Chem. Soc.*, 2005; **127**: 12162-63.

[26] Y. Cakmak, S. Kolemen, S. Duman, Y. Dede, Y. Dolen, B. Kilic, Z. Kostereli, L. T. Yildirim, A. L. Dogan, D. Guc and E. U. Akkaya, *Angew. Chem. Int. Ed. Engl.*, 2011; **50**: 11937-41.

[27] W. Hu, X. F. Zhang, X. Lu, S. Lan, D. Tian, T. Li, L. Wang, S. Zhao, M. Feng and J. Zhang, *Dyes Pigment.*, 2018; **149**: 306-14.

[28] X. F. Zhang and N. Feng, *Chem. Asian J.*, 2017; **12**: 2447-56.

[29] X. F. Zhang and N. Feng, *Spectrochim Acta A: Mol. Biomol. Spectrosc.*, 2018; **189**: 13-21.

[30] D. D. Perrin and W. L. F. Armatego, *Purification of Laboratory Chemicals, 3rd. ed.*, Pergamon Press, New York, 1988.

[31] H. G. O. Becker, W. Berger, G. Domschke, E. Fanghänel, J. Faust, M. Fischer, F. Gentz, K. Gewald, R. Gluch, R. Mayer, K. Müller, D. Pavel, H. Schmidt, K. Schollberg, K. Schwetlick, E. Seiler and G. Zeppenfeld, *Organikum, 20. Aufl., J. A. Barth Verlag*, Heidelberg, Leipzig, 1996.

[32] X. F. Zhang, J. Zhang and L. Liu, *J. Fluoresc.*, 2014; **24**: 819-26.

[33] M. G. Lagorio, L. E. Dicelio, E. A. S. Roman and S. E. J. Braslavsky, *Photochem. Photobiol. B*, 1989; **3**: 615-24.

[34] Y. Cakmak, S. Kolemen, S. Duman, Y. Dede, Y. Dolen, B. Kilic, Z. Kostereli, L. T. Yildirim, A. L. Dogan, D. Guc and E. U. Akkaya, *Angew. Chem. Int. Ed. Engl.*, 2011; **50**: 11937-41.

[35] N. Adarsh, R. R. Avirah and D. Ramaiah, *Org. Lett.*, 2010; **12**: 5720-3.

[36] N. Epelde-Elezcano, V. Martínez-Martínez, E. Peña-Cabrera, C. F. A. Gómez-Durán, I. López Arbeloa I and S. Lacombe, *RSC Adv.*, 2016; **6**: 41991-8.

[37] Ş. Işık and Y. Köysal, *Acta Crystallogr. E*, 2006; **62**: 671-2.

[38] E. Vos de Wael, J. A. Pardoen, J. A. van Koeveringe and J. Lugtenburg, *Recl. Trav. Chim. Pays-Bas*, 1977; **96**: 306-9.

[39] A. Treibs and F. H. Kreuzer, *Ann. Chem.*, 1968; **718**: 208-23.

Highlights

- Eight new charge transfer (CT)-based BODIPY photosensitizers are synthesized.
- The CT efficiency is adjusted by adding 0 to 4 methoxys on meso-phenyl.
- The increase in either the number of methoxys or solvent polarity enhances $^1O_2$ formation.
- Higher CT efficiency favors higher singlet oxygen generation quantum yield.